This is an accepted version. Please find publisher version at doi.org/10.1111/sms.14434

# Electromyography-informed musculoskeletal modelling provides new insight into hand tendon forces during tennis forehand

Goislard de Monsabert, Benjamin[a]* ; Herbaut, Alexis[b] ; Cartier, Théo[a] ; Vigouroux, Laurent[a].

[a]*Aix-Marseille University, CNRS, ISM, Marseille, France;* [b]*Human Factors & Ergonomics Department, Decathlon SportsLab Research and Development, Lille, France*

*Corresponding author:

Benjamin Goislard de Monsabert, Ph.D.

UMR 7287 CNRS & Aix-Marseille University
Faculty of Sport Science, CP 910
163 av. de Luminy
13288 Marseille cedex 09 FRANCE
E-mail: benjamin.goislard-de-monsabert@univ-amu.fr.

**Section**

Biomechanics and Motor Control

This is an accepted version. Please find publisher version at doi.org/10.1111/sms.14434

# Electromyography-informed musculoskeletal modelling provides new insight into hand tendon forces during tennis forehand drive

## Abstract

Lateral epicondylitis, also known as tennis elbow, is a major health issue among tennis players. This musculoskeletal disorder affects hand extensor tendons, results in substantial pain and impairments for sporting and everyday activities and requires several weeks of recovery. Unfortunately, prevention remains limited by the lack of data regarding biomechanical risk factors, especially because in vivo evaluation of hand tendon forces currently remains challenging. Electromyography-informed musculoskeletal modelling is a non-invasive approach to provide physiological estimation of tendon forces based on motion capture and electromyography but was never applied to study hand tendon loading during tennis playing. The objective of this study was to develop such electromyography-informed musculoskeletal model to provide new insight into hand tendon loading in tennis players. The model was tested with three-dimensional kinematics and electromyography data of two players performing forehand drives at two shot speeds and with three rackets. Muscle forces increased with shot speed but were moderately affected by racket properties. Wrist prime extensors withstood among the highest forces, but their relative implication compared to flexors depended on the player-specific grip force and racket motion strategy. When normalising wrist extensor forces by shot speed and grip strength, up to three-fold differences were observed between players, suggesting that gesture technique, e.g., grip position or joint motion coordination, could play a role in the overloading of wrist extensor tendons. This study provided a new methodology for in situ analysis of hand biomechanical loadings during tennis gesture and shed a new light on lateral epicondylitis risk factors.

Keywords: Tennis; lateral epicondylitis; muscle force; musculoskeletal model; motion capture; electromyography

This is an accepted version. Please find publisher version at doi.org/10.1111/sms.14434

## Introduction

Tennis involves both highly dynamic and accurate gestures to intercept and hit the ball to reach a specific target on the opponent's field. This sport places high loads on the joints and muscles of the players that are repeated hundreds of times during each match, hence exposing players to injuries. While the lower limbs of tennis players are affected by acute injuries, e.g., ankle sprain, their upper limb are more affected by chronic overuse syndromes, with lateral epicondylitis (LE), also known as tennis elbow, being the most prevalent affections[1]. LE is affecting the tendon of wrist radial extensors, i.e., the *extensor carpi radialis brevis* (ECRB) and *longus* (ERCL), as well as in some cases those of finger extensors, i.e., *extensor digitorum communis* (EDC)[2]. The pathology incidence is around 30-50% among tennis players[1] and results in substantial pain and impairments for everyday life[3,4] as well as modified muscle coordination during gripping[5]. Understanding the factors inducing LE thus appears crucial to reduce injuries.

The mechanism of LE has been associated to repetitive microtrauma of the tendons progressively initiating an angio-fibroblastic degeneration[6]. Although LE is multifactorial, biomechanical risk factors, such as awkward joint angulations and high tendon tensile forces, are believed to induce tendon damage outside of its optimal physiological re-modelling capacities and accelerate degenerative processes[4,7,8]. One of the central mechanism of LE is that hand extensors tendons are indeed highly involved during gripping activities because the wrist joint balance requires high co-contraction levels[9–11]. Nevertheless, the data regarding hand biomechanical loading during tennis playing remain scarce. The main reason is that the *in vivo* evaluation of tendon forces currently remains challenging for biomechanician since direct measures are highly invasive. Furthermore, indirect measurements, such as forces at the hand/handle interface and joint kinetics, are challenging to obtain in complex motions as tennis

This is an accepted version. Please find publisher version at doi.org/10.1111/sms.14434

gestures and without disturbing the player. Consequently, hand muscle/tendon loading has mainly been inferred from either grip force, wrist net moment, or electromyography (EMG) recordings.

Grip force was assessed either by using pressure sensors equipped on the handle[12] or the hand[13] or by replacing the handle with a dynamometer[14]. Those studies observed a single-peak curve with the highest values, around 200-300N, occurring just before the impact. The instrumentation however required to equip the handle with sensors altering the hand/racket interface thus potentially affecting the player's natural gesture. Removing force sensors is possible by using EMG to estimate grip force[15–17] and was used to study the role of grip force in modulating shock vibration transmission[18]. Despite representing crucial information on the forces at the hand/handle interface, the grip force is the result of the action of over 30 muscles which implication also depends on the mechanical demands at the wrist[19].

Net joint moments, reflecting mechanical load balanced by muscles, can be quantified via inverse dynamics approaches relying on accurate measurement of segment kinematics and inertial parameters of body segment. Such approaches were used to study the upper limb during tennis playing and a few studies provided values at the wrist during serve[20–22] and during the forehand[12,23]. Those studies showed that both flexion-extension (FE) and radial-ulnar deviation (RUD) are facing high torques with values around 5-15 Nm and reaching sometimes 30 Nm, thus similar to maximal isometric contraction performances[24]. Authors also showed that the distribution of the wrist torque between the two degrees of freedom can vary importantly according to the player's individual technique, with for instance larger RUD torques in professional players and larger FE torques in intermediate ones[23]. Although the net moment traduces

This is an accepted version. Please find publisher version at doi.org/10.1111/sms.14434

the overall mechanical demand at the joint, it does not allow to characterize how forces are shared across individual muscles.

EMG analyses during tennis playing demonstrated wrist extensors are among the most implicated forearm muscles during both backhand[25–29] and forehand[30–33] drives. This high activity was observed around the impact and corresponded to the need for muscle actions to balance the increase in wrist mechanical loading associated to both variations of racket dynamics and player's grip force, necessary to control racket orientation and absorb ball/racket impact vibrations. Nevertheless, EMG is not linearly related to the tendon forces and hence cannot fully explain injury mechanisms.

Although previous works informed on grip forces, net joint moment and muscle electrical activity during tennis playing, understanding the biomechanical risks of tendinopathies such as LE requires an approach that allows characterizing forces withstood by hand and wrist muscle-tendon units. Musculoskeletal models represent the only non-invasive method to quantify internal mechanics in complex musculoskeletal systems, such as the hand. Some models rely on a forward-dynamics approach and estimate muscle force from EMG using muscle contraction models. Only one study used such technique to estimate ECRB mechanics during tennis gesture to investigate the influence of skill level[34] but the model was derived from a thumb muscle, whereas hand/forearm muscles present specific mechanical behaviours[35,36]. Other models rely on an inverse-dynamics approach and estimate muscle loading from kinematics and external force data using multibody rigid mechanics and optimization technique[37]. Our group used such an approach to estimate hand extensor loading during tennis forehand and showed that racket handle size might represent a way to modulate this loading to potentially reduce the risk of LE[12]. Nevertheless, the muscle force estimation was only based on kinematics or kinetics data while it has been shown that guiding the muscle

This is an accepted version. Please find publisher version at doi.org/10.1111/sms.14434

load sharing optimisation using EMG data provides a better estimation of muscle co-contraction[38,39]. The development of such EMG-informed models appears crucial to quantify internal loading during tennis gestures and provide new insight on the potential risk of musculoskeletal disorders such as LE.

The objective of this study was thus to propose a method to characterise hand biomechanical loading and estimate hand tendon forces during forehand drives using an EMG-informed musculoskeletal model. A previously developed multibody rigid model of the hand[10] was adapted to study dynamical tasks and to include an EMG guidance at two levels: grip force estimation and muscle load sharing optimisation. The grip force during tennis gestures was estimated from the EMG signal of the *flexor digitorum superficialis* (FDS) based on a player-specific calibration avoiding instrumentation of the racket and minimising perturbation of player gesture. The EMG guidance in the muscle load sharing optimisation consisted in a force-tracking constraint for three muscles (ECRB, EDC and *flexor carpi radialis*: FCR) using previously developed force-length-activation relationships[35,36]. The method was evaluated using motion capture and EMG data measured of two players with different levels and grip position performing forehand drives at two shot speeds and with three rackets.

## Methods

### *Participants*

Two right-handed men with similar anthropometrics volunteered for the study: an Advanced player (ITN 3; Age: 19y; Height 185cm: Weight: 64kg Hand length: 19.7cm) and an Intermediate player (ITN 7; Age: 19y; Height: 183cm; Weight: 73kg Hand length: 20.4cm). The two players used different grip position during forehand, meaning the palmar side of their second metacarpal head was in contact with a different

This is an accepted version. Please find publisher version at doi.org/10.1111/sms.14434

bevel of the racket handle, thus resulting in specific wrist and forearm at impact. The Advanced player used an eastern grip position, i.e., using the bevel parallel to the racket head plane, whereas the Intermediate used a semi-western grip, i.e., using the adjacent bevel in the little finger direction, oriented at 45° of the racket head plane. Both players did not suffer from any injuries within the past 24 months and signed an informed consent before beginning the experiment. The protocol was approved by the local ethics committee of Aix-Marseille University.

***Experimental protocol***

Each player participated in a three-step protocol over a single session (Figure 1). The first step consisted in the electromyography setting-up, including the placement of electrodes and normalisation contraction. The second step concerned grip calibration tasks to determine a relationship between FDS muscle activation and grip force as well as participant-specific maximal grip force, finger joint postures and grip force distribution. Finally, the third step consisted in forehand tasks where upper limb and racket kinematics and EMG activities were recorded to estimate biomechanical loadings during forehand drives.

This is an accepted version. Please find publisher version at doi.org/10.1111/sms.14434

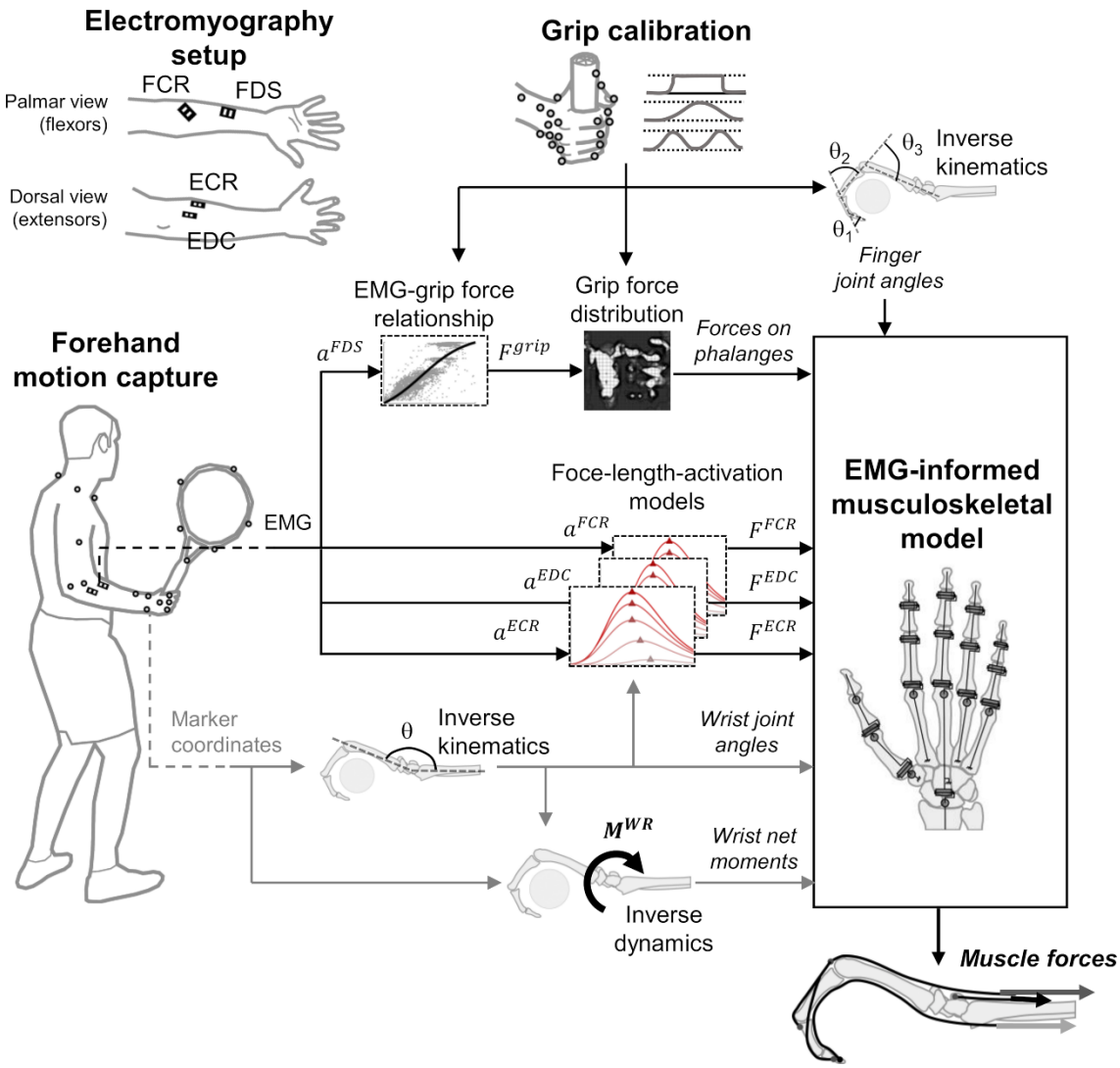


*Figure 1. Framework to estimate muscle forces during forehand drives from forehand and grip calibration data using the EMG-informed musculoskeletal model.*

*Electromyography setting-up*

The activities of four muscles (ECRB; EDC; Flexor Carpi Radialis: FCR; Flexor Digitorum Superficialis: FDS) were recorded during both grip calibration and forehand tasks using a wireless EMG system (Trigno, Delsys, Natick, MA, 2000 Hz) Before placing electrodes, the skin was shaved, sanded and rinsed with an alcoholic solution. The placement of the electrodes followed those established to use previously developed EMG-informed force-length-activation models[35,36]. Functional contractions were used to ensure crosstalk was minimised and included finger flexion and extension, wrist flexion and extension, grip force exertion and radial deviation. After equipment, each

This is an accepted version. Please find publisher version at doi.org/10.1111/sms.14434

participant performed an isometric maximal voluntary contraction consisting in producing a maximal wrist extension moment while firmly gripping a racket handle for normalisation purposes of ECRB and EDC EMG signals. Participants were encouraged verbally. Participants performed two trials separated by a 2-minute rest. No additional maximal contraction was performed for flexors normalisation purpose as grip calibration tasks already included maximal force exertions.

*Grip calibration*

*Task.* Participants performed isometric grip force tracking tasks. During each trial, both the target time-force curve and their current force-time curve were plotted on a screen. Their instruction was to follow the target profile as closely as possible. The participants were standing and were instructed to position their fingers on the handle the same way they grip the racket during forehand drives. The upper limb posture was let free to perform the task in a comfortable way while ensuring the optical markers (see below) were seen by cameras.

*Protocol.* First, each participant performed three maximum grip force trials with the instruction of reaching the maximal value as fast as possible and maintaining that level for 5 seconds. No target force-time curve was plotted, and participants were encouraged verbally. The maximal RMS value (50-ms window) of all three trials was taken as a maximal force reference to scale all the other tasks. Participants then performed the grip force tracking tasks following three types of target curve: constant, single-sine, double-sine. During constant trials, participants aimed at maintaining for 5s a grip force level indicated by a horizontal line positioned. The three force levels tested were 75%, 50% and 25% of the subject maximal force. During single-sine curve, the participants had to follow a force-time curve describing first a 3s constant force and then a sine cycle

(increase and decrease) over a period of 10s starting and ending at the level of the initial constant level. The amplitude of the sine was 25% of the maximal force reference with a beginning either at 5, 15 or 30 % of the subject maximal force, hence corresponding to three grip force ranges, i.e., 5-30%, 15-40%, 30-55%. During double-sine, the participants performed the same task as the single-sine, except that, after the initial level, the target curve described two sine cycles over the 10-s period. The same amplitude and initial levels were used as in single-sine trials. Each task was repeated twice for a total of 18 trials (3 tasks × 3 force levels × 2 trials) separated by a 30-sec rest. Task and repetitions were randomised for each participant.

*Material.* The systems to record grip force and hand kinematics were the same as in a previous study[10]. Grip force was recorded at 2000 Hz with a cylindrical dynamometer (3.3-cm diameter, Sixaxes, Argenteuil, FR). The dynamometer is divided into 6 beams, each equipped with strain gauge sensors and was mounted on a mechanical arm which helped participants maintaining the upper limb posture, but which could move slightly to prevent applying any unrequired mechanical actions, such as pulling or pronation moment. The grip force distribution across hand segments was assessed using a pressure sensor map (Hoof 3200F-scan mobile; TekScan, Boston, MA, 50Hz). The pressure map consisting in 1089 transducers (33 rows by 33 columns, 0.5-cm spacing) each having a 0-255 range was wrapped around the handle, and they were both squeezed during all trials. Finger segment kinematics were tracked using a motion capture system consisting of seven cameras (MX T40, Vicon, Oxford, UK, 100Hz) tracking 29 reflective markers placed on the dorsal aspects of the forearm and the hand (Figure s1-4 and Table s1-1 in Electronic Supplementary Material ESM1). Muscle activity of FDS was recorded as mentioned in above section. An external trigger was used to synchronise the acquisition of all four recording systems.

This is an accepted version. Please find publisher version at doi.org/10.1111/sms.14434

*Forehand task*

*Task.* The forehand task was inspired from previous works of our group[12]. Participants were instructed to hit a target with a ball using a flat forehand drive, i.e., with as less top spin as possible. The target was a 50-cm square located at 1.5m from the ground fixed and fixed on a large net used to cushion the ball shock. The participant was facing the target, standing 6m away from it and was instructed to move as less as possible in both frontal and lateral directions. The balls were sent by a ball machine at 2.5 m/s (Tennis twist, Sports Tutor, Burbank, CA) positioned at the net level and 3m on the left side of the target. The ball machine was adjusted to ensure participants could hit the ball after one rebound with minimal displacements.

*Protocol.* Participants performed the forehand task described above with three different rackets and at two different shot speeds. The properties of the three rackets are presented in Table 1. The R2w racket is the same model as R2 but with a 15-g added weight on the top. The R1 racket was chosen because of its light weight and lower moment of inertia values. Participants were instructed to perform the forehand task using either the minimal or maximal shot speed, further called “Slow” and “Fast”, allowing them to repeatably reach the target. Those speeds were adjusted by the participants for the first tested racket and the participants were instructed to reproduce them as closely as possible for the following rackets. To allow those adjustments, the participants hit approximately 40 balls when a new racket condition was presented. Racket order was randomised, and the speed conditions were randomised within each racket condition. For each shot speed with a racket, five trials were recorded.

*Material.* Upper limb and racket kinematics were assessed using again a same seven-camera motion capture system (MX T40, Vicon, Oxford, UK) tracking 20 reflective

This is an accepted version. Please find publisher version at doi.org/10.1111/sms.14434

markers placed on upper trunk, arm, forearm, and hand of right upper limb (Figure s2-4 and Table s2-1 in Electronic Supplementary Material ESM2). For each participant, five balls covered with reflective tape were used to track the ball position during recorded trials. Muscle activities of FCR, ECR, FDS, and EDC were recorded at 2000Hz (see "Electromyography setting-up" section for details). EMG signals were synchronously recorded with kinematic data using an external trigger.

*Table 1. Properties of the three rackets used during the study.*

| | R1 | R2 | R2w* |
|---|---|---|---|
| Model | Décathlon TR560 2017 | Décathlon TR990 2017 | Décathlon TR990 2017 |
| String Tension (kg) | 25/23 | 25/23 | 25/23 |
| Handle Size | 3 | 3 | 3 |
| Length (mm) | 680 | 685 | 685 |
| Balance[a] (mm) | 344 | 323 | 340 |
| Mass (g) | 270 | 305 | 320 |
| Polar MOI[b] (Mg/mm²) | 1.34 | 1.39 | 1.40 |
| Transverse MOI[b] (Mg/mm²) | 12.5 | 14.3 | 16.2 |
| Lateral MOI[b] (Mg/mm²) | 13.9 | 15.7 | 17.6 |

*R2w is the same racket as R2 with an added 15-g weight at the racket top. [a]The balance corresponds to the distance from the handle extremity to the centre of mass along the longitudinal axis. [b]MOI: moment of inertia.

### *Forehand kinematics*

#### *Kinematic data processing*

The kinematics of the racket, ball and upper limb were determined from marker coordinates during forehand trials. For each trial, a 1.5-s analysis window centred around the ball impact time frame was first determined and kept for further analysis. The impact frame was considered as the minimal 3D relative distance between the ball and the racket centre, calculated as the mean of the two side markers, using raw coordinates. The marker coordinates were low-pass filtered (Butterworth, 5Hz, order 2, zero-phase). Because of its discontinuous trajectory, the ball coordinates before and after impact frame were filtered separately and the raw coordinates at impact were kept as the position at impact.

This is an accepted version. Please find publisher version at doi.org/10.1111/sms.14434

*Performance indexes*

The performance during forehand drives was analysed qualitatively using racket trajectory and quantitatively using racket and ball velocities. The racket trajectory was plotted in the transverse and sagittal planes using the racket centre position at impact as origin. The racket centre and ball velocities and accelerations were obtained through central differentiation from filtered marker coordinates using one frame before and one frame after the current frame and low-pass filtering (Butterworth, 5Hz, order 2, zero-phase) after each step of differentiation. Inbound ($V_{in}^{ball}$ and $V_{in}^{rack}$) and outbound ($V_{out}^{ball}$ and $V_{out}^{rack}$) ball and racket velocities were determined by averaging their norm on the window going from 25 to 5 frames before and 5 frames to 25 frames after the impact frame. The after/before ratio of the ball and racket velocities were also determined.

*Upper limb joint angles*

The upper limb joint angles were estimated from the filtered marker coordinates on the impact-centred window. The wrist was described by two degrees of freedom (DoF) in flexion/extension and radial/ulnar deviation, the forearm by one DoF in pronation/supination and the elbow by one DoF in flexion/extension. At each time frame, segment coordinate systems were determined, and the joint angles were extracted from relative orientation matrices using Cardan sequences (see Table s2-2 and corpus of Electronic Supplementary Material 2, ESM2). Flexion, pronation and ulnar deviation angle correspond to positive value.

*Finger posture on the handle*

The posture of the fingers on the handle during forehand drives was considered constant during the forehand motion and was extracted from the position of reflective markers during the grip calibration protocol. The marker coordinates were averaged on

This is an accepted version. Please find publisher version at doi.org/10.1111/sms.14434

100 frames when the participant was exerting a grip force on the handle. For the Advanced player, the data was taken from a maximum grip force trial. For the Intermediate player, not all markers could be seen on maximum grip trials, so the marker coordinates were taken during a 15-40% single sine trial. The finger posture was characterised by 23 joint angles calculated using a previously developed method[10]. The trapeziometacarpal (TMC) and metacarpophalangeal (MCP) joints were described by two DoF in flexion/extension and radial/ulnar deviation and the proximal (PIP) and distal (DIP) joints by one DoF in flexion/extension. For each joint, a distal and a proximal segment coordinate system were calculated from marker positions (see Table s1-2 and corpus of Electronic Supplementary Material ESM1) and joint angles were extracted from the relative orientation matrix using a Z-Y-X (flexion/pronation/abduction) sequence of Cardan angles. Flexion, and ulnar deviation angle correspond to positive value.

### *Hand biomechanical loadings during forehand*

#### *Muscle activation*

The muscle activation was calculated from EMG signals the same way for both protocols. For each muscle, the signal was processed to be used with our force-length-activation relationships[35] with first the application of a bandpass filter (Butterworth, 10-400Hz, order 2, zero-phase) and then obtaining EMG envelope by rectifying and applying a lowpass filter (Butterworth, 5Hz, order 2, zero-phase). The muscle activation was then calculated by normalizing each envelope value in a trial by the maximal envelope value observed among all trials for that muscle, i.e., both MVC, grip calibration and forehand drives.

This is an accepted version. Please find publisher version at doi.org/10.1111/sms.14434

*Grip force*

The grip force during forehand drives was estimated from FDS muscle activation using a player-specific relationship derived from grip calibration experimental data, i.e., dynamometer and EMG. First, the six signals from the dynamometer were low-pass filtered (Butterworth, 5Hz, order 2, zero-phase) and converted to Newtons via a calibration matrix. The grip force was then computed as the sum from the six forces recorded by the beams of the dynamometer and normalised by the maximal grip force (MGF), determined as the maximal RMS value (500-ms window) among the three maximum grip trials performed at the beginning of the grip calibration session. The FDS activation was calculated the same way as explained above. For each trial, only the data corresponding to the points where normalised grip force was higher than 5% were kept and FDS muscle activation and grip force were then linearly interpolated to obtain 200 data points for a total of 3600 points of each signal (18 trials).

The EMG to grip force relationship was a sigmoid function (equation 1) which parameters were estimated by a constrained least square optimisation (*fmincon*, MATLAB R2021b) aiming to minimise the squared difference between measured ($f^{grip}$) and estimated ($\hat{f}^{grip}$) grip force (equation 2). The criterion and sigmoid function were as follows:

$$\hat{f}^{grip}(a^{FDS}) = K \cdot \left(\frac{1}{1+e^{-\beta\cdot(a^{FDS}-a_0)}} - 0.5\right) + f_0 \quad (1)$$

$$G(f_0, a_0, K, \beta) = \sum_t \left(f^{grip}(t) - \hat{f}^{grip}(a^{FDS})\right)^2 \quad (2)$$

Where $t$ represents a time sample, $a^{FDS}$ is the muscle activation of FDS, and $\boldsymbol{p} = \{f_0, a_0, K, \beta\}$ are the parameters of the sigmoid relationship. The optimisation included boundaries on parameters, i.e., $0 \leq a_0 \leq 1$, $0 \leq f_0 \leq 1$, $1.01 \leq K \leq 10$, $0.1 \leq \beta \leq$

This is an accepted version. Please find publisher version at doi.org/10.1111/sms.14434

10. Two supplementary constraints regarding the value of estimated grip force for activation at 0 and 1, i.e., $\hat{f}^{grip}(0) = 0$ and $\hat{f}^{grip}(1) = 1$.

*Grip force distribution in the hand*

The grip force distribution across hand segments during forehand drives was estimated for each player using the pressure sensor data measured during the grip calibration session using a previously developed method[10]. The pressure data was taken from the 75% constant force task, using only the trial with the highest maximal value. Briefly, a single pressure map was obtained by averaging each of the 1089 transducer signal on a 500-ms window corresponding to the maximal 500-ms RMS value of the grip force. The pressure map was then normalised by dividing each transducer value by the sum of all transducer values. From this normalised pressure map, 25 normalised forces were obtained by manually segmenting the pressure map to identify 25 anatomical areas, i.e., five by fingers. Each normalised force was computed as the sum of the normalised transducer values within the corresponding segmented area. The force applied on an anatomical area during forehand drive is obtained by multiplying the normalised force by the estimated grip force.

*Wrist net moment*

The wrist moment was determined from the racket and upper limb marker coordinates recorded during the forehand drives using a Newton-Euler inverse dynamics method. The hand and racket were considered as a single rigid body. The hand-racket system inertial properties were deduced from those of the racket (Table 1) and the hand. The hand mass was estimated from participant's hand length, width as well as hand and wrist circumferences using regression equations[40]. Because those equations assume a "flat" hand posture, with straight fingers, the hand centre of mass

This is an accepted version. Please find publisher version at doi.org/10.1111/sms.14434

(CoM) and inertia were determined differently assuming the hand as a cylinder wrapping around the racket handle. The hand CoM was the projection of the 3rd metacarpal head marker on the racket longitudinal axis. The hand inertia was determined by assuming a cylinder whose internal diameter was the racket diameter (Table 1). The cylinder inter-radii distance was equal to the distance between the 3rd metacarpal head marker and the hand CoM. The cylinder length was equal to the participant's hand width. The hand-racket system CoM (G) was then determined as the weighted average of the two points, i.e., considering their mass. The inertia matrices were rotated to the hand-racket coordinate system and translated to the hand-racket CoM. The intersegmental force and moment of the hand-racket system on the radius were then determined:

$$\boldsymbol{F^{WR}} = m\boldsymbol{a} - m\boldsymbol{g} \quad (3)$$

$$\boldsymbol{M^{WR}} = [\boldsymbol{I}^G]\dot{\boldsymbol{\omega}} + \boldsymbol{\omega} \times [\boldsymbol{I}^G]\boldsymbol{\omega} - \boldsymbol{d} \times \boldsymbol{F^{WR}} \quad (4)$$

Where $\boldsymbol{F_{WR}}$ and $\boldsymbol{M_{WR}}$ are the intersegmental force and moment, $\boldsymbol{a}$ and $\boldsymbol{\omega}$ are the linear and angular velocities of the system, $m$ is the mass, $\boldsymbol{g}$ the gravity vector, $[\boldsymbol{I}^G]$ is the inertia matrix expressed at the CoM and $\boldsymbol{d}$ is the vector going from the CoM to the wrist joint centre calculated as the unweighted barycentre of the ulnar and radial styloid markers. The wrist intersegmental moment was then rotated to the radius coordinate system. The ball-racket impact force was not considered in these calculations.

*Estimation of muscles forces*

The muscle forces during forehand drives were determined via an EMG-informed musculoskeletal model adapted from a previous study[10]. Briefly, this model considers the musculoskeletal chains of the wrist and the five fingers by included 21

This is an accepted version. Please find publisher version at doi.org/10.1111/sms.14434

rigid segments (three phalanges and one metacarpal per long finger, two phalanges, one metacarpal and the trapezium for the thumb and the radius). The segments were linked by 23 DoF, with one rotation for the nine interphalangeal joints, two rotations for the five metacarpophalangeal joints, the trapeziometacarpal joint and the wrist joints. The DoFs were actuated by 42 muscle-tendon units, including 18 hand intrinsic muscles, 18 extrinsic and 6 wrist prime movers[10]. The list of all muscles is provided in Table s3-1 of Electronic Supplementary 3 (ESM3).

The 42 muscle forces were estimated using a static optimization procedure aiming to minimise muscle stress (equation 5) while ensuring mechanical equilibrium (equation 6) and respecting EMG-informed muscle force constraints and extensor mechanism force transmission constraints. The muscle stress criterion and mechanical equilibrium were described as follows:

$$J(\boldsymbol{F^M}) = \sum_m \left(\frac{F^m}{PCSA^m}\right)^4 \quad (5)$$

$$[\mathbf{R^M}]\boldsymbol{F^M} + \boldsymbol{M^E} + \boldsymbol{M^P} = \mathbf{0} \quad (6)$$

Where $\boldsymbol{F^M}$is the 42×1 muscle force vector, $PCSA^m$ is the physiological cross sectional area of a muscle, $[\mathbf{R^M}]$ is a 23×42 matrix describing moment arm of each muscle at all DoF calculated from finger posture and wrist joint angle, $\boldsymbol{M^E}$ is the 23×1 external moment vector including the wrist moment calculated above (equation 3) and those calculated from the forces acting on phalanges deduced from grip force level and force distribution data (see above), $\boldsymbol{M^P}$ is a 23×1 vector including moments of passive structures at the TMC and MCP joints. Phalanx segment lengths, points describing tendon path of the finger muscle-tendon units and their PCSA were scaled using hand length and hand breadth. The action of extrinsic finger muscles was included in the

This is an accepted version. Please find publisher version at doi.org/10.1111/sms.14434

wrist balance mechanical equilibrium. The force distribution in the extensor mechanism was also solved in the optimisation procedure using constraints equation. More details on the data and calculations described above can be found in our previous study[10].

In addition to constraints regarding mechanical equilibrium (equation 6) and extensor mechanism, the optimization procedure was guided by constraining the forces of FCR, ECRB and the four EDC comportments to be equal to an EMG-informed estimation of muscle force. This EMG-informed estimation was based on muscle-specific force-length-activation relationships experimentally derived from in vivo motion capture data and already presented in previous studies[9,35,36]. Electronic Supplementary Material 3 (ESM3) provide additional results (Figure s3-2 and s3-3), parameters (Table s3-2 to s3-7) and methodological details (Figure s3-7) of these EMG-informed estimations. Briefly, the current muscle-tendon length is first estimated from wrist and finger joint angles using geometric models. The muscle length due to active contraction is deduced from muscle-tendon length and muscle activation. Finally, muscle force is estimated from muscle length and activation using a force-length relationship considering a non-linear activation-dependency of the maximal isometric force, optimal length, and shape of the curve.

To reduce computational time, the muscle forces were estimated on five specific time frames related to racket motion, illustrated on Figure s2-2 of Electronic Supplementary Material ESM2 and corresponding to :

- Beginning of forward acceleration: first frame where antero-posterior component of racket velocity in the laboratory frame is positive, i.e., toward the net, on the 1.5-s window kinematic analysis.

- Peak racket forward acceleration: frame corresponding to maximal value of antero-posterior component of racket acceleration in the laboratory frame before impact frame
- Pre-Impact: three frames before the ball-racket impact
- Peak racket vertical acceleration: frame corresponding to maximal value of vertical component of racket acceleration in the laboratory frame after impact frame
- End of forward acceleration: last frame where antero-posterior component of racket velocity in the laboratory frame is positive, i.e., toward the net, on the 1.5-s window kinematic analysis.

The static optimisation procedure was run for the five frames of interest mentioned above using as input the time-varying wrist joint angles and moments (equation 3) and grip force level and fixed finger posture and grip force distribution in the hand (see above for details).

To provide a global understanding of tendon loadings, the 42 muscle forces were reduced to 4 muscle group forces, namely wrist prime extensors (W-ext; including Ecu, ECRB and ECRL), wrist prime flexors (W-flex; including PL, FCR and FCU), finger extrinsic extensors (F-ext; including the four compartments of EDC) and finger extrinsic flexors (F-flex; including the four compartments of FDS and FDP). Each group muscle force is the sum of the individual muscle forces in the group. The results of the 42 individual forces are provided in Figure s3-4 and s3-5 Electronic Supplementary Material 3 (ESM3).

This is an accepted version. Please find publisher version at doi.org/10.1111/sms.14434

### *Data analysis*

The analysis aimed at studying the influence of shot speed (Slow vs Fast) and racket properties (R1 vs R2 vs R2w) on hand biomechanical loading data and identify differences between players, e.g., due to skill level or general gesture technique. For comparison between players, kinetic variables were normalised and expressed as percentage of MGF for grip force and muscle forces or of the product of MGF and hand length (HL) for wrist net moment. To express the kinetic and muscle efficiency of each player gesture, the percentage-normalised values were divided by the ball velocity after impact ($V_{out}^{ball}$) in m/s[21]. A low efficiency index value corresponds to a greater efficiency. The comparisons will not include statistical tests as only two players were analysed and only five repetitions per condition were acquired.

## Results

### *Grip force calibration results*

All results associated with the grip calibration protocol (relationship between grip force and electromyography, grip force distribution and finger posture) are presented in Figures s1-1, s1-2 and s1-3 of Electronic Supplementary Material ESM1. A brief description of the key elements will be provided here. The measured MGF was 653.2 N and 1195.2 N for the Advanced and the Intermediate player, respectively. The estimated grip force obtained from FDS activation, with the player-specific least-square fitted relationship (equation 1), correlated well with experimental data ($R^2$=0.87 for Advanced; $R^2$=0.82 for Intermediate). The average root mean square error (RMSE) calculated from all estimated and experimental values was moderate (RMSE = 9% of MGF for Advanced and RMSE = 12% of MGF for Intermediate player).

This is an accepted version. Please find publisher version at doi.org/10.1111/sms.14434

### *Forehand performance*

The forehand performance indexes related to racket and ball velocities are presented in Table 2. The inbound ball velocity was approximately 2.3 m/s and similar across shot speeds, racket properties, and players. The outbound ball velocity $V_{ball}^{out}$ was influenced by speed shots and was approximately 10 m/s higher during Fast speed shots compared to Slow ones and were slightly lower for the Advanced player than for the Intermediate. The results suggest an influence of racket properties on on $V_{ball}^{out}$. For the Advanced player, the use of R2 resulted in slightly higher velocities for both shot speeds and the use of R1 resulted in lower velocities during Fast shots. For the Intermediate player, the use of R2w resulted in slightly lower velocities during Slow shots.

*Table 2. Mean ± one standard deviation values (N=5 trials) of racket and ball velocities before (in) and after (out) the ball/racket impact of both players (Advanced and Intermediate) for each of the two shot speeds (Slow, Fast) performed with one of the three rackets (R1, R2 R2w)*

| | Ball velocity | | | Racket velocity | | |
|---|---|---|---|---|---|---|
| | $V_{ball}^{in}$(m/s) | $V_{ball}^{out}$(m/s) | $V_{ball}^{out}/V_{ball}^{in}$ | $V_{rack}^{in}$ (m/s) | $V_{rack}^{out}$ (m/s) | $V_{rack}^{out}/V_{rack}^{in}$ |
| Advanced player | | | | | | |
| Slow | | | | | | |
| R1 | 2.4 ± 0.2 | 12.3 ± 0.5 | 5.2 ± 0.4 | 5.6 ± 0.4 | 2.9 ± 0.4 | 0.5 ± 0.1 |
| R2 | 2.4 ± 0.2 | **15.0 ± 0.4 ⁜** | 6.2 ± 0.4 | 6.4 ± 0.2 | 3.0 ± 0.3 | 0.5 ± 0.0 |
| R2w | 2.4 ± 0.2 | 13.3 ± 0.7 | 5.5 ± 0.3 | 6.0 ± 0.3 | 3.0 ± 0.3 | 0.5 ± 0.0 |
| Fast | | | | | | |
| R1 | 2.3 ± 0.2 | ***23.7 ± 2.0 #*** | 10.2 ± 1.5 | 8.2 ± 0.6 | 4.1 ± 0.1 | 0.5 ± 0.0 |
| R2 | 2.4 ± 0.1 | **26.4 ± 0.9 ⁜** | 11.0 ± 0.4 | 8.8 ± 0.4 | 4.6 ± 0.3 | 0.5 ± 0.0 |
| R2w | 2.2 ± 0.2 | 25.7 ± 1.2 | 11.6 ± 1.0 | 8.5 ± 0.2 | 4.1 ± 0.4 | 0.5 ± 0.1 |
| Intermediate player | | | | | | |
| Slow | | | | | | |
| R1 | 2.3 ± 0.2 | 20.4 ± 2.4 | 8.8 ± 1.6 | 7.6 ± 0.6 | 3.0 ± 0.6 | 0.4 ± 0.1 |
| R2 | 2.3 ± 0.1 | 20.2 ± 2.3 | 8.7 ± 1.1 | 7.4 ± 0.7 | 3.0 ± 0.7 | 0.4 ± 0.1 |
| R2w | 2.3 ± 0.1 | ***18.5 ± 1.7 #*** | 8.0 ± 0.7 | 6.9 ± 0.5 | 2.9 ± 0.4 | 0.4 ± 0.1 |
| Fast | | | | | | |
| R1 | 2.4 ± 0.1 | ***28.5 ± 0.9 #*** | 12.1 ± 0.5 | 8.1 ± 0.3 | 5.1 ± 0.5 | 0.6 ± 0.1 |
| R2 | 2.3 ± 0.1 | 31.1 ± 1.4 | 13.3 ± 0.7 | 9.0 ± 0.3 | 5.6 ± 0.4 | 0.6 ± 0.1 |
| R2w | 2.2 ± 0.2 | 31.0 ± 2.4 | 14.1 ± 0.4 | 8.8 ± 0.1 | 5.2 ± 0.4 | 0.6 ± 0.1 |

Bold font and ⁜ symbol highlight a high value across the three rackets. Bold italic font and # symbol highlight a low value across the three rackets

This is an accepted version. Please find publisher version at doi.org/10.1111/sms.14434

The inbound racket velocity ($V_{rack}^{in}$) was influenced by shot speeds, with an increase of approximately 2.5 and 1.5 m/s during Fast shots for Advanced and Intermediate player, respectively. Inbound and outbound racket velocities were not influenced by racket properties.

Electronic Supplementary Material ESM2 provides additional graphics presenting racket trajectories (Figure s2-1) and time-patterns of racket (Figure 2-2) and joint kinematics (Figure s3-3).

### *Hand biomechanical loadings during forehand*

*Forearm muscle activation*

The muscle activation time-patterns during forehand drives measured using EMG are presented in Figure 2. The shot speed influenced activation levels with globally higher peak values during Fast shots, except for EDC. For the Advanced player, the greatest increases were around 20% for the wrist extensor (ECR) and the finger flexors (FDS). For the Intermediate player the greatest increase in maximal activation level was for the wrist flexor (FCR) with around 40% higher maximal values during Fast shots. The ECR activation time-pattern of the Advanced player also changed from a single peak during Slow shots to a double peak during Fast shots. The racket properties had no influence on muscle activation pattern of the Advanced player. For the Intermediate player, the use of the R2w led to a decrease of FCR activation during Slow shots and an increase of FDS activation during Fast shots compared to other rackets. The comparison of players suggested different timing of muscle activations relative to ball/racket impact and different muscle coordination. Compared to the Intermediate player, the Advanced player peak activation values were reached earlier, and the muscle coordination suggested lower wrist (FCR) and finger (FDS)

This is an accepted version. Please find publisher version at doi.org/10.1111/sms.14434

flexors activation levels and higher activation levels of wrist extensor (ECR) during Fast shots.

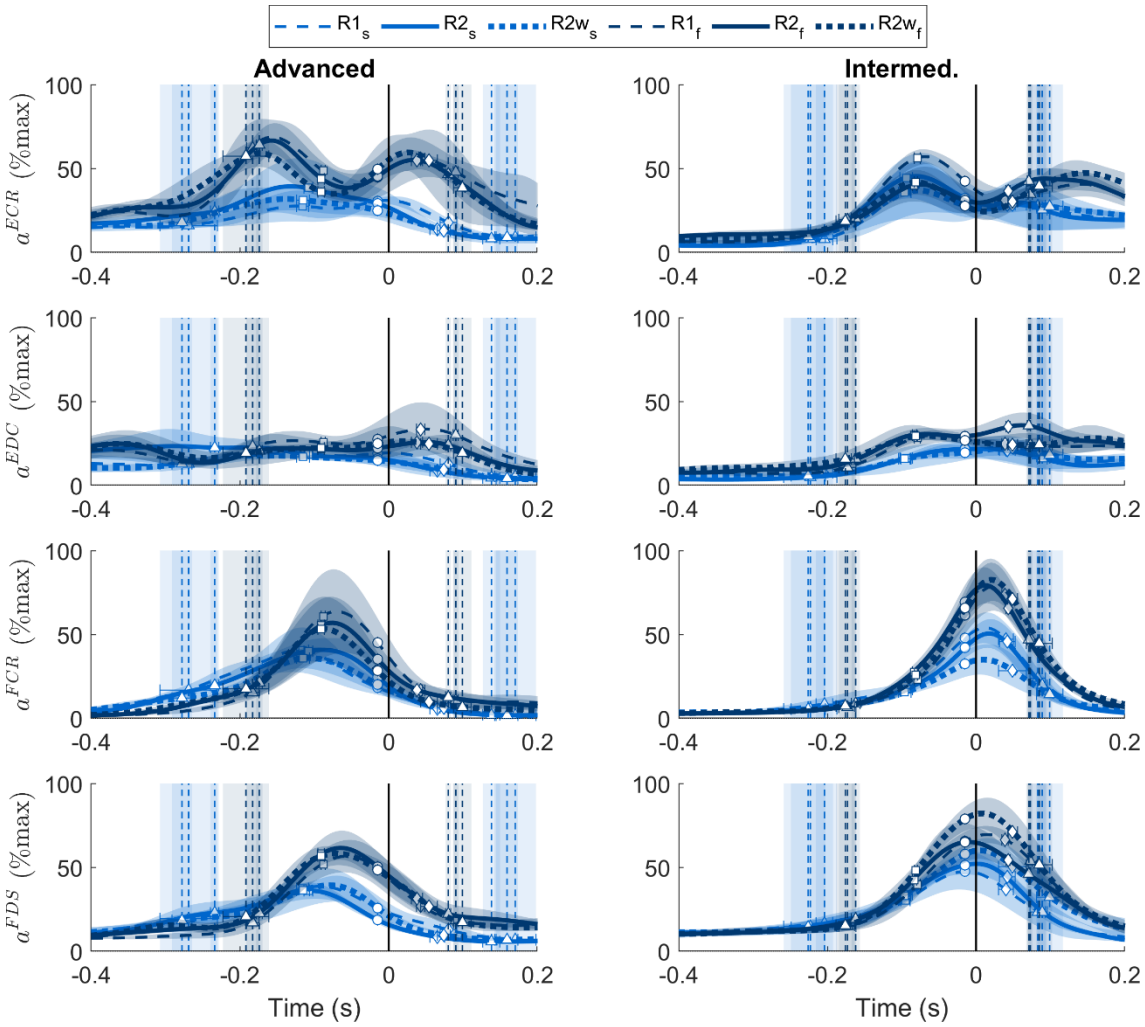


*Figure 2. Mean time-patterns (N=5 trials) of muscle activations during the forehand drive of both players (Advanced and Intermediate) for the two shot speeds (Slow; Fast) performed with the three rackets (R1, R2, R2w). Shaded areas represent ± one standard deviation around the mean. Lighter nuances represent the Slow (s) speed shots, and darker nuances the Fast (f) ones. The vertical solid black bar represents the impact frame, the dashed vertical bars represent the beginning and end of forward acceleration phase, and the different points correspond to the frames on which musculoskeletal model was run (see corpus). ECR: Extensor Carpi Radialis, EDC: Extensor Digitorum Communis, FCR: Flexor Carpi Radialis, FDS: Flexor Digitorum Superficialis.*

This is an accepted version. Please find publisher version at doi.org/10.1111/sms.14434

*Grip force*

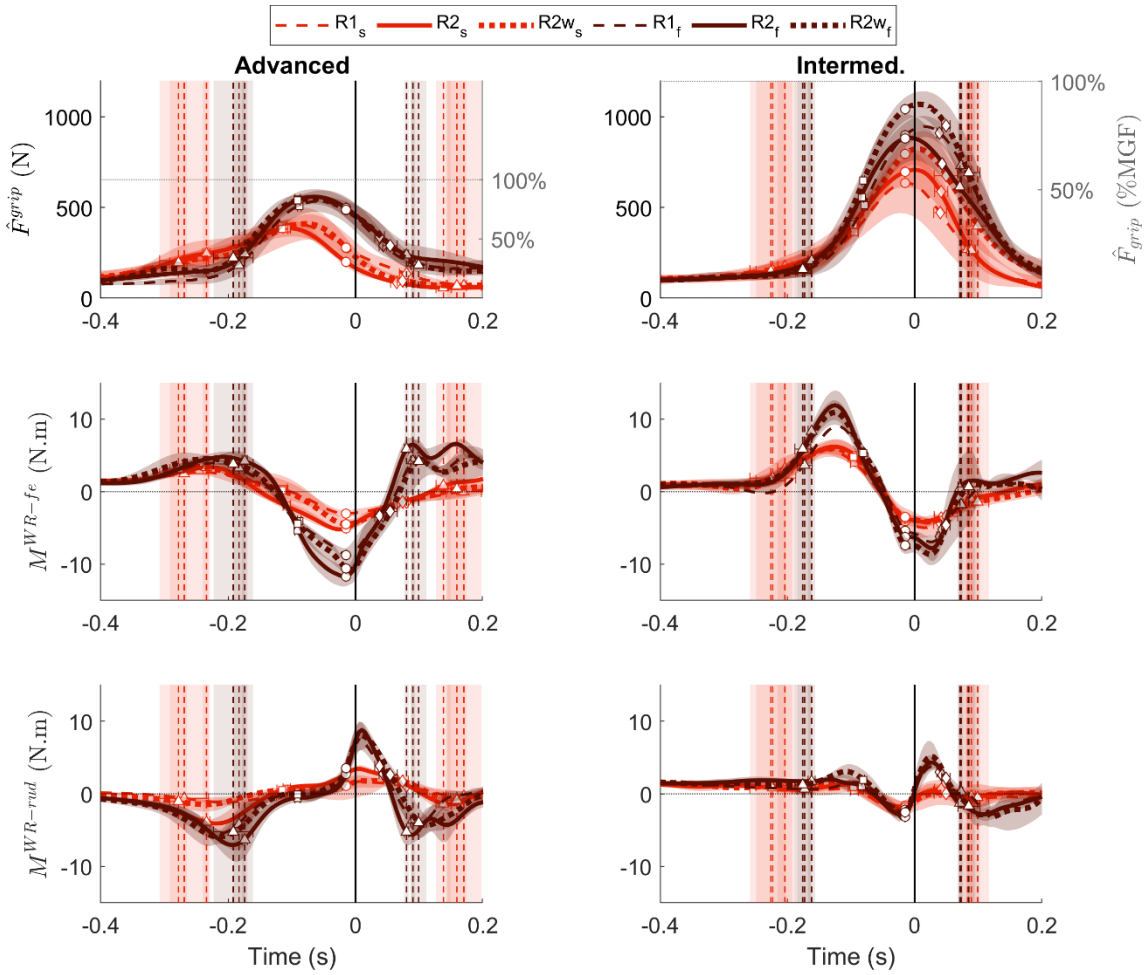


*Figure 3. Mean time-patterns (N=5 trials) of estimated grip force ($\hat{F}^{grip}$) and wrist flexion/extension ($M^{WR-fe}$) and radial-ulnar deviation ($M^{WR-rud}$) moments during the forehand drives of both players (Advanced and Intermediate) for the two shot speeds (Slow and Fast) performed with the three rackets (R1, R2, R2w). Shaded areas represent ± one standard deviation around the mean. Lighter nuances represent the Slow (s) speed shots and darker nuances the Fast (f) ones. The vertical solid black bar represents the impact frame, the dashed vertical bars represent the beginning and end of forward acceleration phase, and the different points correspond to the frames on which musculoskeletal model was run (see corpus). Normalised $\hat{F}^{grip}$ values expressed in percentage of maximal grip force (MGF) are represented on the right axis of upper panels. Wrist moment components are expressed from an internal point of view, such that positive values represent a flexion and ulnar moment exerted by muscles.*

The estimated grip force during forehand drives estimated from FDS activation are presented in Figure 3 and Table 3. The shot speed influenced grip force with higher forces during Fast shots. At Pre-Impact, this increase was up to 40% and 20% for the

This is an accepted version. Please find publisher version at doi.org/10.1111/sms.14434

Advanced and Intermediate players, respectively. The racket properties influenced the grip force with a decrease of 10% for the Advanced player using R2 during slow shots and an increase of 10% for the Intermediate player using the R2w.

*Table 3. Mean ± one standard deviation values of estimated grip force ($\hat{F}^{grip}$) and wrist flexion/extension ($M^{WR-fe}$) and radial-ulnar deviation ($M^{WR-rud}$) moments at the Pre-Impact time (three frames before impact) for both players (Advanced and Intermediate) for each of the two shot speeds (Slow and Fast) performed with one of the three rackets (R1, R2, R2w)*

| Kinetics at Pre-Impact | | Normalised value (%$MGF$ or %$MGF \cdot HL$) | | Efficiency index (%/$V_{ball}^{out}$) | |
|---|---|---|---|---|---|
| | | Slow | Fast | Slow | Fast |
| $\hat{F}^{grip}$ | | | | | |
| | Advanced | | | | |
| | R1 | 42.4 ± 12.1 | 74.4 ± 11.1 | 3.47 ± 1.06 | 3.13 ± 0.32 |
| | R2 | ***30.6 ± 3.9 #*** | 76.1 ± 8.1 | ***2.04 ± 0.26 #*** | 2.88 ± 0.29 |
| | R2w | 42.6 ± 8.2 | 74.6 ± 7.1 | 3.21 ± 0.70 | 2.90 ± 0.26 |
| | Intermediate | | | | |
| | R1 | 53.1 ± 14.1 | 75.2 ± 5.7 | 2.58 ± 0.43 | 2.63 ± 0.15 |
| | R2 | 58.3 ± 7.1 | 73.7 ± 11.3 | 2.89 ± 0.15 | 2.37 ± 0.34 |
| | R2w | **66.5 ± 6.4 ⁑** | **87.2 ± 5.4 ⁑** | **3.63 ± 0.54 ⁑** | **2.84 ± 0.41 ⁑** |
| $M^{WR-fe}$ | | | | | |
| | Advanced | | | | |
| | R1 | ***-2.4 ± 0.4 #*** | ***-6.8 ± 0.7 #*** | ***-0.19 ± 0.03 #*** | ***-0.29 ± 0.01 #*** |
| | R2 | -3.9 ± 0.3 | **-9.1 ± 1.0 ⁑** | -0.26 ± 0.02 | **-0.34 ± 0.03 ⁑** |
| | R2w | -3.5 ± 0.6 | -8.2 ± 0.7 | -0.26 ± 0.04 | -0.32 ± 0.02 |
| | Intermediate | | | | |
| | R1 | -1.7 ± 0.5 | -2.2 ± 0.2 | -0.08 ± 0.02 | -0.08 ± 0.01 |
| | R2 | -1.5 ± 0.2 | -2.6 ± 0.1 | -0.08 ± 0.02 | -0.08 ± 0.00 |
| | R2w | -1.4 ± 0.5 | -3.0 ± 0.5 | -0.08 ± 0.03 | -0.10 ± 0.01 |
| $M^{WR-rud}$ | | | | | |
| | Advanced | | | | |
| | R1 | 1.0 ± 0.6 | 2.7 ± 1.0 | 0.08 ± 0.05 | 0.11 ± 0.04 |
| | R2 | **2.1 ± 0.3 ⁑** | ***2.1 ± 1.3 #*** | **0.14 ± 0.02 ⁑** | ***0.08 ± 0.05 #*** |
| | R2w | 0.8 ± 1.5 | 2.7 ± 1.2 | 0.06 ± 0.11 | 0.11 ± 0.04 |
| | Intermediate | | | | |
| | R1 | -0.9 ± 0.3 | -0.9 ± 0.2 | -0.04 ± 0.01 | -0.03 ± 0.01 |
| | R2 | -0.7 ± 0.2 | -1.3 ± 0.2 | -0.03 ± 0.01 | -0.04 ± 0.01 |
| | R2w | -0.8 ± 0.4 | -1.0 ± 0.1 | -0.04 ± 0.03 | -0.03 ± 0.01 |

Normalised forces are expressed as percentage of maximal grip force (MGF) and moments as percentage of the product of MGF and hand length (HL). Efficiency is the percentage-normalised value divided by ball velocity after impact ($V_{ball}^{out}$) in m/s. Bold font and ⁑ symbol highlight a high value across the three rackets. Bold italic font and # symbol highlight a low value across the three rackets

The grip force efficiency index at Pre-Impact was not influenced by shot speed or player technique but showed some differences between rackets (Table 3). The efficiency index was lower for the Advanced player using R2 during Slow shots and higher for the Intermediate player using R2w.

*Wrist moment*

The components of wrist moment during forehand drives calculated from marker coordinates are presented in Figure 3 and Table 3. The shot speed influenced the maximal intensities of both wrist moment components with higher peak values during Fast shots. The racket properties had no influence on flexion-extension and radial-ulnar moments of the Intermediate player. For the Advanced player, the use of racket R2 modified intensities of wrist moments at Pre-Impact with a lower radial-ulnar moment and a higher flexion-extension moment during Fast shots and higher radial-ulnar moment Slow shots (Table 3). The use of R1 for that same player resulted in a slightly lower extension moment intensities at Pre-Impact (Table 3). The comparison of players showed differences in temporal evolution and intensities of both wrist moment components as well as differences in the direction of the radial-ulnar moment. The peak flexion moment value close to the beginning of forward acceleration was lower and reached earlier for the Advanced player. The peak extension moment value during Fast shots around the impact was higher and reached earlier for the Advanced player. The peak radial-ulnar deviation moment values were higher for the Advanced player. At the beginning of the forward acceleration, the advanced player produced a peak radial moment whereas the Intermediate player produced a constant ulnar moment.

The wrist moment efficiency indexes at Pre-Impact were not influenced by shot speed or racket properties for the Intermediate player (Table 3). For the Advanced player, only the extension moment efficiency index changed between speed shots, presenting higher, suggesting less efficient kinetic strategy, during Fast shots. The ulnar moment efficiency index of the Advanced player was higher, suggesting less efficient kinetic strategy, when using R2 during Fast shots. The comparison of players demonstrated that the Advanced player was using a less efficient kinetic strategy with values two to four times higher than for the Intermediate player.

This is an accepted version. Please find publisher version at doi.org/10.1111/sms.14434

***Hand muscle forces during forehand drive***

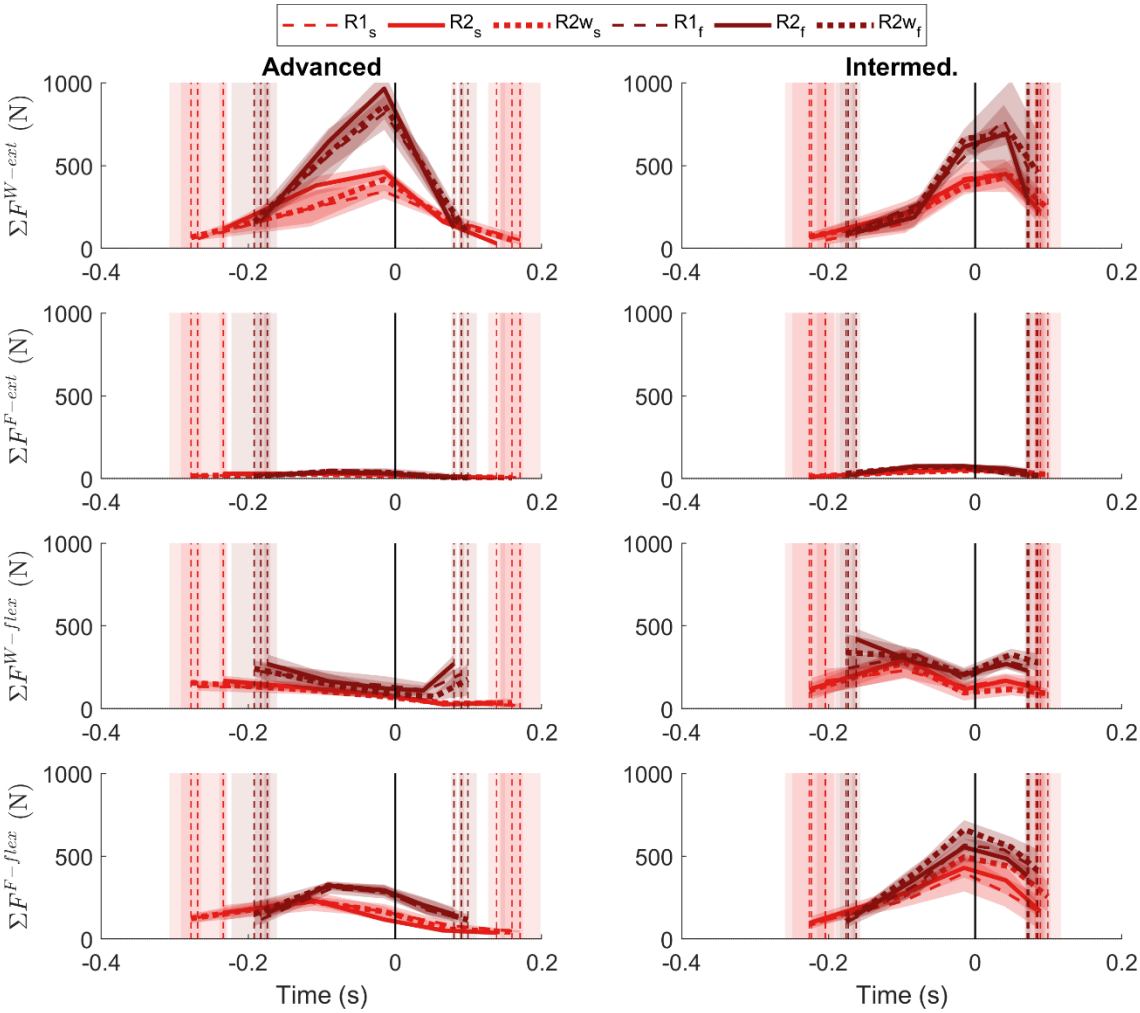


*Figure 4. Mean time-patterns (N=5 trials) of estimated muscle forces ($\sum F^m$) during the forehand drives of both players (Advanced and Intermediate) for the two shot speeds (Slow and Fast) performed with the three rackets (R1, R2, R2w). Shaded areas represent ± one standard deviation around the mean. Lighter nuances represent the Slow (s) speed shots and darker nuances the Fast (f) ones. The vertical solid black bar represents the impact frame, the dashed vertical bars represent the beginning and end of forward acceleration phase (see corpus). W-ext: wrist extensors (ECRB, ECRL, ECU); F-ext: finger extensors (four compartments of EDC); W-flex: wrist flexors (FCR, FCU, PL); F-flex: finger flexors (four compartments of FDS and four compartments of FDP)*

The hand muscle group forces during forehand drives estimated using the musculoskeletal model are presented in Figure 4 and Table 4. The shot speed influenced muscle forces with higher values at Pre-Impact during Fast shots, except for the finger

extensors F-ext. For the Advanced player, these increases were more pronounced for the wrist extensors (W-ext) and finger flexors (F-flex) with up to twice higher values than during Slow shots. For the Intermediate player, the muscle force increase reached less important values and was more evenly distributed across muscle groups, from about 35% for finger flexors to 75% for wrist flexors. The racket properties had no influence on F-ext and W-flex forces and influenced forces of other muscle groups differently for each player. For the Advanced player, the use of R2 increased W-ext force during Fast shots and reduced F-flex force during Slow shots. For the Intermediate player, the use of R2w increased W-ext muscle force during Fast shots and F-flex muscle forces for both shot speeds. The comparison of players suggested different muscle coordination. Compared to the Intermediate player, the Advanced player presented higher muscle forces of W-ext during Fast shots and lower W-flex and F-flex muscle forces for both speeds.

The muscle force efficiency index at Pre-Impact was not influenced by shot speed for the Intermediate player (Table 3). For the Advanced player, only the muscle force efficiency index of W-ext changed between shot speeds, presenting higher values, suggesting a less efficient strategy, during Fast shots. The influence of racket properties was different for each player. When the advanced player used R2, the muscle force efficiency of W-ext was higher, suggesting a less efficient strategy, during Fast shots and that of F-flex was lower, suggesting a more efficient strategy, during Slow shots. When the Intermediate player used R2w, the muscle force efficiency of W-ext and F-flex were higher, suggesting a less efficient strategy, during Fast and Slow shots, respectively. The comparison of players showed that the Advanced player presented three times higher W-ext efficiency index, suggesting a less efficient strategy.

This is an accepted version. Please find publisher version at doi.org/10.1111/sms.14434

Additional graphics presenting time-patterns of individual muscle forces are presented in Figures s3-4 and s3-5 of Electronic Supplementary Material ESM3.

*Table 4. Mean ± one standard deviation values of estimated muscle group forces ($\sum F^m$) at Pre-Impact (three frames before impact) for both players (Advanced and Intermediate) for each of the two shot speeds (Slow and Fast) performed with the three rackets (R1, R2, R2w)*

| Muscle forces at Pre-impact | | Normalised value ($\%MGF$) | | Efficiency index ($\%/V_{ball}^{out}$) | |
|---|---|---|---|---|---|
| | | Slow | Fast | Slow | Fast |
| $\sum F^{W-ext}$ | | | | | |
| | Advanced | | | | |
| | R1 | 52.6 ± 6.4 | 125.0 ± 15.5 | 4.3 ± 0.5 | 5.3 ± 0.4 |
| | R2 | 70.8 ± 6.2 | **147.6 ± 15.2 ⁑** | 4.7 ± 0.4 | **5.6 ± 0.6 ⁑** |
| | R2w | 63.9 ± 10.6 | 132.3 ± 12.6 | 4.8 ± 0.7 | 5.1 ± 0.3 |
| | Intermediate | | | | |
| | R1 | 35.3 ± 8.0 | 46.1 ± 4.3 | 1.7 ± 0.2 | 1.6 ± 0.1 |
| | R2 | 34.1 ± 4.0 | 51.3 ± 4.9 | 1.7 ± 0.2 | 1.6 ± 0.2 |
| | R2w | 31.0 ± 2.4 | **55.4 ± 4.9 ⁑** | 1.7 ± 0.3 | **1.8 ± 0.2 ⁑** |
| $\sum F^{F-ext}$ | | | | | |
| | Advanced | | | | |
| | R1 | 3.8 ± 1.2 | 6.9 ± 2.7 | 0.3 ± 0.1 | 0.3 ± 0.1 |
| | R2 | 3.6 ± 1.4 | 4.9 ± 1.5 | 0.2 ± 0.1 | 0.2 ± 0.1 |
| | R2w | 3.1 ± 0.4 | 5.8 ± 2.8 | 0.2 ± 0.0 | 0.2 ± 0.1 |
| | Intermediate | | | | |
| | R1 | 4.7 ± 1.3 | 6.0 ± 0.6 | 0.2 ± 0.0 | 0.2 ± 0.0 |
| | R2 | 4.5 ± 1.3 | 6.3 ± 0.5 | 0.2 ± 0.0 | 0.2 ± 0.0 |
| | R2w | 4.1 ± 0.9 | 5.8 ± 0.9 | 0.2 ± 0.0 | 0.2 ± 0.0 |
| $\sum F^{W-flex}$ | | | | | |
| | Advanced | | | | |
| | R1 | 11.2 ± 1.5 | 21.8 ± 8.4 | 0.9 ± 0.1 | 0.9 ± 0.3 |
| | R2 | 12.8 ± 2.6 | 18.9 ± 6.1 | 0.9 ± 0.2 | 0.7 ± 0.2 |
| | R2w | 11.3 ± 1.7 | 14.5 ± 4.9 | 0.8 ± 0.1 | 0.6 ± 0.2 |
| | Intermediate | | | | |
| | R1 | 11.3 ± 2.4 | 14.8 ± 4.1 | 0.6 ± 0.1 | 0.5 ± 0.1 |
| | R2 | 9.8 ± 3.1 | 17.3 ± 2.7 | 0.5 ± 0.2 | 0.5 ± 0.1 |
| | R2w | 8.1 ± 3.9 | 17.3 ± 3.5 | 0.4 ± 0.2 | 0.6 ± 0.1 |
| $\sum F^{F-flex}$ | | | | | |
| | Advanced | | | | |
| | R1 | 25.1 ± 7.2 | 43.8 ± 6.5 | 2.1 ± 0.6 | 1.8 ± 0.2 |
| | R2 | ***18.0 ± 2.2 #*** | 45.0 ± 4.9 | ***1.2 ± 0.1 #*** | 1.7 ± 0.2 |
| | R2w | 25.2 ± 4.9 | 44.0 ± 4.4 | 1.9 ± 0.4 | 1.7 ± 0.2 |
| | Intermediate | | | | |
| | R1 | 33.3 ± 9.3 | 47.5 ± 3.1 | 1.6 ± 0.3 | 1.7 ± 0.1 |
| | R2 | 35.9 ± 4.9 | 46.4 ± 7.4 | 1.8 ± 0.1 | 1.5 ± 0.2 |
| | R2w | **41.4 ± 4.3 ⁑** | **55.3 ± 4.7 ⁑** | **2.3 ± 0.3 ⁑** | **1.8 ± 0.3 ⁑** |

Normalised forces are expressed as percentage of maximal grip force (MGF). Efficiency is the percentage-normalised value divided by ball velocity after impact ($V_{ball}^{out}$) in m/s. Bold font and ⁑ symbol highlight a high value across the three rackets. Bold italic font and # symbol highlight a low value across the three rackets. W-ext : wrist extensors (ECRB, ECRL, ECU); F-ext : finger extensors (four compartments of EDC); W-flex : wrist flexors (FCR, FCU, PL); F-flex : finger flexors (four compartments of FDS and four compartments of FDP)

## Discussion

This study aimed at quantifying hand extensor tendon forces, often affected by lateral epicondylalgia, during tennis gestures based on a methodology combining

motion capture, electromyography, and musculoskeletal modelling. The use of motion capture and electromyography provided an in vivo evaluation of grip force and wrist moment, as well as tendon forces, while avoiding invasive sensors that perturb the player gesture or modify racket properties. The methodology was tested with two players performing forehand drives with three rackets and two different speed shots. The results suggest the methodology provides physiologically realistic estimation of hand biomechanical loadings. The study also shows that muscle forces during forehand drives seemed more influenced by shot speed or player-specific technique than racket properties. The loadings withstood by wrist extensors were the highest among the main hand muscle groups and were modulated by both the grip force and wrist moment that varies according to player's technique, e.g., racket motion dynamics and grip position.

Despite a lack of data and a variability of assessment methods in the literature, the hand biomechanical loading values obtained using the present methodology were consistent with other works. As already observed before in EMG analysis of the forehand, ECR and FCR activation reached similar peak levels[33] in the acceleration phase or early follow-through[32]. Contrary to a previous study[32], EDC activation remained stable and low. However, little information was provided in this early work on the instruction regarding how players performed forehand drives, e.g., ball speed or accuracy constraints, such that it is difficult to understand this difference. FDS activation during forehand has never been evaluated but the time-pattern of its envelope is consistent with previous recordings of grip force, with a peak around the impact time[12–14]. The maximal grip force estimated from FDS activation demonstrated a similar time-pattern than in previous works but reached higher absolute levels than previous works, up to 1000N against 200-300 N[12,14]. The higher values can be explained by different measurement tools. The MGF was measured using a six-beam handle in the

present study whereas previous evaluations relied on pressure map and unidirectional dynamometer which underestimate grip forces[10]. Finally, wrist moment intensities were also comparable to a previous evaluation during forehand drives, i.e., values between 5 and 15 N.m at Pre-impact[23]. Those relatively good agreements with the literature confirm the hand biomechanical loading estimated with the present methodology are physiologically realistic.

***Influence of shot speed on hand biomechanical loadings***

The results showed that, for the two analysed players, a higher shot speed increased the grip force exerted by the player as well as wrist moment due to racket motion dynamics (Figure 3 and Table 3) and resulted in higher hand tendon forces (Figure 4 and Table 4). These increases could be expected as the players increased by about 30% the inbound racket velocity during Fast shots compared to Slow ones (Table 2). As a result, the wrist moment increased because of the higher linear and angular inertial moments resulting from greater accelerations of the hand-racket system before impact. The player also exerted around 30% higher grip force during Fast shots, probably in an effort to maintain racket motion stability, compensating for increased accelerations and anticipating greater ball/racket impact forces. With higher wrist moments and grip forces, the muscle forces estimated by the musculoskeletal model also increased with shot speed, but this increase was spread differently across muscle groups for each player. Fast shots led to a two-fold increase of wrist extensor loading for the Advanced player whereas it led to lesser and more evenly distributed variations across all muscle group forces for the Intermediate player (+35 to +75%). This difference between players can be explained by a modification of the gesture efficiency. The efficiency indexes indeed showed that, for a same outbound ball velocity, the Advanced player withstood a greater extension moment during Fast shots (Table 3) that

This is an accepted version. Please find publisher version at doi.org/10.1111/sms.14434

resulted in higher wrist extensor forces (Table 4), suggesting a less efficient strategy than during Slow shots. On the contrary, the efficiency indexes of the Intermediate player remained relatively stable across shot speeds (Table 3 and 4), suggesting a similar gesture strategy between shot speeds resulting in a scaling of mechanical loadings with performance. The degradation of the Advanced player gesture efficiency could be explained by the fact that the difference between the racket velocities of his Slow and Fast shots was higher (40%) than for the Intermediate player (20%). Because of this larger difference in speed, the Advanced player significantly changed his joint motion coordination whereas the Intermediate player moderately changed it (see time-pattern of joint angles in Figure s2-3 of Electronic Supplementary Materials ESM2). Those results suggest the adjustments of hand biomechanical loading to shot speed are not necessarily linear and that considering this gesture parameter is necessary to fully understand the wrist and finger muscle forces associated with tennis gesture.

***Influence of racket properties on hand biomechanical loadings***

The results showed that racket properties had a relatively low influence on hand biomechanical loadings for the two analysed players with different trends between players. For the Intermediate player, the efficiency indexes suggested that, for a given shot speed, the use of R2w increased the finger flexor muscle force (Figure 4 and Table 4). This result could be explained by the fact that R2w racket is the heaviest (Table 1) and might thus require a firmer grip to ensure a proper control of its trajectory and orientation at impact which is confirmed with higher grip force indexes (Table 3). As the wrist moment intensities were equivalent, the data suggest the Intermediate player maintained similar racket and joint motion dynamics but had to increase its grip force to face the higher weight of the racket. The R2w racket appears inappropriate for the Intermediate player compared to other rackets as, for a given speed, it resulted in a

supplementary load on finger flexors that could potentially lead to fatigue or musculoskeletal disorders. For the Advanced player, the use of racket R2 appears to have modified its hand biomechanical loading but the trend is unclear. With this racket, the finger flexor force was lower during Slow shots and the wrist extensor force was higher during Fast shots. The reason for these adjustments can be explained by the fact the use of R2 resulted in a lower grip force during Slow shots and a higher wrist flexion-extension moment intensities during Fast shots. Nevertheless, the fact that the trend was not constant across shot speeds and influenced different muscle groups does not allow to conclude on whether the R2 racket is suited for the Advanced player. Furthermore, the R2 racket is neither the lightest nor the heaviest racket nor possesses extreme moments of inertia values compared to other rackets (Table 1) such that no rationale can be found on the influence on muscle force. The use of R1 also resulted in unclear trends for the Advanced player as it modified the wrist moment intensities but not muscle forces. Overall, the changes in hand biomechanical loadings resulting from different racket use during forehand appears marginal despite large variations in racket weights (from 270 for R1 to 320 g for R2w). A previous study identified that the polar moment could significantly influence wrist moment components[22] but these differences were observed during the serve motion where the racket motion dynamics are much higher than in the current study, i.e., Pre-Impact racket speed of 22m/s against 8m/s here. Beyond these differences with literature, only two players were considered so that no trend can be directly expressed from our results and further studies are required to understand the effect of racket properties on wrist and finger muscle forces and potentially confirm whether this effect is player specific.

***Influence of player technique on hand biomechanical loadings***

The results indicated that the Advanced player muscle force coordination was less efficient than the one of the Intermediate Player with a much higher contribution of wrist extensor muscles (Table 4). The efficiency indexes indicated that, for a given speed shot and considering maximal grip force capacity, the wrist extensor muscle forces of the Advanced player were 2.5 to 3.5 five times higher than those of the Intermediate player. This inefficient coordination of the Advanced player does not result from grip force efficiency, which was comparable with the Intermediate player, but from the upper limb and racket motion dynamics which affected the wrist flexion-extension moment, which was 3.5 times higher once normalised by muscle capacities and shot speed. This higher wrist moment intensities observed for the Advanced player resulted from the larger amplitudes of elbow flexion-extension and forearm prono-supination (Figure s2-3 in Electronic Supplementary Materials ESM2) increasing the inertial effects of the angular acceleration of the hand racket system (see time-pattern of wrist moment components in Figure s3-1 of Electronic Supplementary Materials ESM3). These increased joint angle amplitudes of the Advanced player probably resulted from his use of an eastern grip while the Intermediate player used a semi-western grip. As already observed by Elliott et al.[41], the use of an eastern grip by the Advanced player involved a greater involvement of elbow extension, increasing the relative distance of the racket, to produce racket speed. On the contrary, by using a semi-western grip, the Intermediate player maintained a more flexed elbow and supinated forearm, keeping the hand closer to the trunk and relying on shoulder internal rotation to develop racket speed. This different joint coordination results in different angular and linear accelerations of the hand-racket system and impact differently the wrist moment components. The results from the present study suggest that an eastern grip position might be less efficient from the hand biomechanical loading point of view,

This is an accepted version. Please find publisher version at doi.org/10.1111/sms.14434

resulting in higher moment intensities at the wrist. More importantly, this inefficiency might negatively impact wrist extensors by increasing their tensile loads and potentially lead to a higher risk of LE[7], confirming the pathology could be related to player's technique[1]. Again, as only two participants were investigated, a larger population will be necessary to elucidate the influence of player-specific grip position and joint coordination on the forces acting on the common extensor tendon. Nevertheless, the use of the EMG-informed musculoskeletal model highlighted that hand tendon loading results from an interplay between the level of grip force wrist moment intensities, both directly implied in the control of racket motion, but that might vary between different players. Those results corroborate the idea that hand muscle coordination is related to both wrist moment and grip force[19].

***Limitations***

Some limitations should be considered when interpreting the results from this study. First, only two players participated in the study to test this methodology so that the trends observed need to be investigated with larger population samples to be confirmed, especially regarding the risk of tendinopathies like LE. Second, the accuracy of the grip force estimation was on average 10% of MGF which is not negligible. Nevertheless, this error is comparable to previous attempts to estimate grip forces from electromyography[15–17] and is inherent to the non-linear relationship between EMG and force. This error remains acceptable considering the use of EMG represents the only alternative way to avoid the use of sensors modifying the hand/racket interface such as dynamometer[14] or force sensitive systems[12,13]. A sensitivity analysis (Figure s3-6 Electronic Supplementary ESM3) showed that the grip force estimation uncertainty mainly modulates the implication of finger extrinsic flexors (FDP and FDS compartments) as well as few intrinsic muscles but not extensor tendon forces. The

This is an accepted version. Please find publisher version at doi.org/10.1111/sms.14434

sensitivity analysis also showed that the muscle load sharing is sensitive to the radial-ulnar deviation moment, so that care should be taken regarding its calculation. Finally, the musculoskeletal model relied on generic muscle capacities, e.g., PCSA, whereas studies showed that tennis playing modifies the hand musculature non-uniformly across hand flexors and extensors[24]. The obtained muscle load sharing could have thus been modified if the musculoskeletal model included player-specific capacities. Nevertheless, obtaining this player-specific muscle strength profile would have required another measurement session, whereas the protocol already lasted two hours and a half on average. The muscle forces estimated through this methodology nevertheless provide a good order of magnitude of the loading withstood by hand muscle tendons during the tennis forehand drive as well as how shot speed, racket properties and player's technique can influence them.

**Perspective**

This study proposed a methodology to evaluate hand biomechanical loading during tennis gesture using motion capture, electromyography, and musculoskeletal modelling. The methodology provided estimations of grip force, wrist moment and muscle forces that were consistent with previous works. The wrist extensors withstood among the highest muscle forces and the total force exerted on the common extensor tendon could reach levels close to 1000N for relatively moderate shot speeds, i.e., outbound ball velocity below 30m/s. Those values confirm wrist extensors are exposed to large amount of force during tennis playing, corroborating their exposure to tendinopathies like LE. Nevertheless, the use of the EMG-informed musculoskeletal model suggests that this loading is modulated by the interplay between the level of grip force and the intensities of the two wrist moment components that depends on player-specific technique, e.g., grip position and joint coordination. Further studies are thus

required to evaluate the role of those player-specific strategies on hand biomechanical loading. The methodology should also be applied to study hand muscle forces during backhand drives which seems associated to abnormal wrist extensor loading[1]. Future works should also attempt to reduce the equipment for both the racket and player to facilitate its use outside laboratory environment.

**Acknowledgements**

The authors would like to thank the participants for their patience and Dr Hugo Hauraix for his assistance during the data acquisition.

**Data availability statement**

The datasets generated and/or analysed during the current study are available from the corresponding author on reasonable request.

**Conflict of interest disclosure**

Part of the study was funded through a research collaboration between the Decathlon company and the Aix-Marseille university. The authors will not receive any financial benefits from the results of this study and declare no competing interest.

**References**

1. Abrams GD, Renstrom PA, Safran MR. Epidemiology of musculoskeletal injury in the tennis player. Br J Sports Med 2012;46:492–498.

2. Fairbank SM, Corlett RJ. The Role of the Extensor Digitorum Communis Muscle in Lateral Epicondylitis. J Hand Surg 2002;27:405–409.

3. De Smedt T, de Jong A, Van Leemput W, Lieven D, Van Glabbeek F. Lateral epicondylitis in tennis: update on aetiology, biomechanics and treatment. Br J Sports Med 2007;41:816–819.

4. Tosti R, Jennings J, Sewards JM. Lateral Epicondylitis of the Elbow. Am J Med 2013;126:357.e1-357.e6.

5. Heales LJ, Bergin MJG, Vicenzino B, Hodges PW. Forearm Muscle Activity in Lateral Epicondylalgia: A Systematic Review with Quantitative Analysis. Sports Med 2016;46:1833–1845.

6. Nirschl RP. Elbow tendinosis/tennis elbow. Clin Sports Med 1992;11:851–870.

7. Keir PJ, Farias Zuniga A, Mulla DM, Somasundram KG. Relationships and Mechanisms Between Occupational Risk Factors and Distal Upper Extremity Disorders. Hum Factors J Hum Factors Ergon Soc 2021;63:5–31.

8. Pizzolato C, Lloyd DG, Barrett RS, Cook JL, Zheng MH, Besier TF, Saxby DJ. Bioinspired Technologies to Connect Musculoskeletal Mechanobiology to the Person for Training and Rehabilitation. Front Comput Neurosci 2017;11:96.

9. Caumes M, Goislard de Monsabert B, Hauraix H, Berton E, Vigouroux L. Complex couplings between joints, muscles and performance: the role of the wrist in grasping. Sci Rep 2019;9:1–11.

10. Goislard de Monsabert B, Rossi J, Berton E, Vigouroux L. Quantification of hand and forearm muscle forces during a maximal power grip task. Med Sci Sports Exerc 2012;44:1906–1916.

11. Snijders CJ, Volkers AC, Mechelse K, Vleeming A. Provocation of epicondylalgia lateralis (tennis elbow) by power grip or pinching. Med Sci Sports Exerc 1987;19:518–523.

12. Rossi J, Vigouroux L, Barla C, Berton E. Potential effects of racket grip size on lateral epicondilalgy risks. Scand J Med Sci Sports 2014;24:e462-470.

13. Knudson DV. Factors affecting force loading on the hand in the tennis forehand. J Sports Med Phys Fitness 1991;31:527–531.

14. Lucki NC, Nicolay CW. Phenotypic plasticity and functional asymmetry in response to grip forces exerted by intercollegiate tennis players. Am J Hum Biol 2007;19:566–577.

15. Claudon L. Evaluation of Grip Force Using Electromyograms in Isometric Isotonic Conditions. Int J Occup Saf Ergon 1998;4:169–184.

16. Hoozemans MJM, van Dieën JH. Prediction of handgrip forces using surface EMG of forearm muscles. J Electromyogr Kinesiol 2005;15:358–366.

17. Keir PJ, Mogk JPM. The development and validation of equations to predict grip force in the workplace: contributions of muscle activity and posture. Ergonomics 2005;48:1243–1259.

18. Chadefaux D, Rao G, Androuet P, Berton E, Vigouroux L. Active tuning of stroke-induced vibrations by tennis players. J Sports Sci 2017;35:1643–1651.

19. Forman DA, Forman GN, Robathan J, Holmes MWR. The influence of simultaneous handgrip and wrist force on forearm muscle activity. J Electromyogr Kinesiol 2019;45:53–60.

20. Martin C, Bideau B, Delamarche P, Kulpa R. Influence of a Prolonged Tennis Match Play on Serve Biomechanics (MA Lebedev, Ed.). PLOS ONE 2016;11:e0159979.

21. Martin C, Bideau B, Ropars M, Delamarche P, Kulpa R. Upper limb joint kinetic analysis during tennis serve: Assessment of competitive level on efficiency and injury risks: Upper limb joint kinetics during tennis serve. Scand J Med Sci Sports 2014;24:700–707.

22. Rogowski I, Creveaux T, Chèze L, Macé P, Dumas R. Effects of the Racket Polar Moment of Inertia on Dominant Upper Limb Joint Moments during Tennis Serve (RJ van Beers, Ed.). PLoS ONE 2014;9:e104785.

23. Bahamonde RE, Knudson D. Kinetics of the upper extremity in the open and square stance tennis forehand. J Sci Med Sport 2003;6:88–101.

24. Vigouroux L, Goislard de Monsabert B, Hayot C, Androuet P, Berton É. Assessment of the risk and biomechanical consequences of lateral epicondylalgia by estimating wrist and finger muscle capacities in tennis players. Sports Biomech 2017;16:434–451.

25. Blackwell JR, Cole KJ. Wrist kinematics differ in expert and novice tennis players performing the backhand stroke: Implications for tennis elbow. J Biomech 1994;27:509–516.

26. Giangarra CE, Conroy B, Jobe FW, Pink M, Perry J. Electromyographic and cinematographic analysis of elbow function in tennis players using single- and double-handed backhand strokes. Am J Sports Med 1993;21:394–399.

27. Glynn JA, Kentel BB, King MA, Mitchell SR. A Comparison of Wrist Angular Kinematics and Forearm EMG Data for an Elite, Intermediate and Novice Standard Tennis Player Performing a One-handed Backhand Groundstroke. Int J Sports Sci Eng 2007;1:157–164.

28. Hatch GF, Pink MM, Mohr KJ, Sethi PM, Jobe FW. The Effect of Tennis Racket Grip Size on Forearm Muscle Firing Patterns. Am J Sports Med 2006;34:1977–1983.

29. Kelley JD, Lombardo SJ, Pink M, Perry J, Giangarra CE. Electromyographic and Cinematographic Analysis of Elbow Function in Tennis Players with Lateral Epicondylitis. Am J Sports Med 1994;22:359–363.

30. Chow JW, Knudson DV, Tillman MD, Andrew DPS. Pre- and post-impact muscle activation in the tennis volley: effects of ball speed, ball size and side of the body. Br J Sports Med 2007;41:754–759.

31. Furuya R, Yokoyama H, Dimic M, Yanai T, Vogt T, Kanosue K. Difference in racket head trajectory and muscle activity between the standard volley and the drop volley in tennis (H Choo, Ed.). PLOS ONE 2021;16:e0257295.

32. Morris M, Jobe FW, Perry J, Pink M, Healy BS. Electromyographic analysis of elbow function in tennis players. Am J Sports Med 1989;17:241–247.

33. Rogowski I, Rouffet D, Lambalot F, Brosseau O, Hautier C. Trunk and Upper Limb Muscle Activation During Flat and Topspin Forehand Drives in Young Tennis Players. J Appl Biomech 2011;27:15–21.

34. Riek S, Chapman AE, Milner T. A simulation of muscle force and internal kinematics of extensor carpi radialis brevis during backhand tennis stroke: implications for injury. Clin Biomech 1999;14:477–483.

35. Goislard de Monsabert B, Hauraix H, Caumes M, Herbaut A, Berton E, Vigouroux L. Modelling force-length-activation relationships of wrist and finger extensor muscles. Med Biol Eng Comput 2020;58:2531–2549.

36. Hauraix H, Goislard De Monsabert B, Herbaut A, Berton E, Vigouroux L. Force–Length Relationship Modeling of Wrist and Finger Flexor Muscles. Med Sci Sports Exerc 2018;50:2311–2321.

37. Blache Y, Creveaux T, Dumas R, Chèze L, Rogowski I. Glenohumeral contact force during flat and topspin tennis forehand drives. Sports Biomech 2017;16:127–142.

38. Hoang HX, Diamond LE, Lloyd DG, Pizzolato C. A calibrated EMG-informed neuromusculoskeletal model can appropriately account for muscle co-contraction in the estimation of hip joint contact forces in people with hip osteoarthritis. J Biomech 2019;83:134–142.

39. Vigouroux L, Quaine F, Labarre-Vila A, Amarantini D, Moutet F. Using EMG data to constrain optimization procedure improves finger tendon tension estimations during static fingertip force production. J Biomech 2007;40:2846–2856.

40. Zatsiorsky VM. Kinetics of human motion. Human Kinetics; 2002. 680 p.

41. Elliott B, Takahashi K, Noffal G. The Influence of Grip Position on Upper Limb Contributions to Racket Head Velocity in a Tennis Forehand. J Appl Biomech 1997;13:182–196.

**Electronic supplementary materials**

Electronic Supplementary Material 1 (ESM1) – PDF File - Results and methodological details of the grip calibration protocol

Electronic Supplementary Material 2 (ESM2) – PDF File - Additional results and methodological details of the forehand motion capture protocol

Electronic Supplementary Material 3 (ESM3) – PDF File - Additional results and methodological details of the musculoskeletal model